Journal of Proteomics 227 (2020) 103902

Contents lists available at ScienceDirect

Journal of Proteomics

journal homepage: www.elsevier.com/locate/jprot

Proteomic analysis of exosomes derived from procyclic and metacyclic-like cultured *Leishmania infantum chagasi*

David M. Forrest[a], Michel Batista[b,c], Fabricio K. Marchini[b,c], Antonio J. Tempone[a], Yara Maria Traub-Cseko[a,*]

[a] Laboratório de Biologia Molecular de Parasitas e Vetores, Instituto Oswaldo Cruz-Fiocruz, Av. Brasil 4365, 21045-900 Rio de Janeiro, RJ, Brazil
[b] Laboratório de Ciências e Tecnologias Aplicadas em Saúde, Instituto Carlos Chagas-Fiocruz, Rua Prof. Algacyr Munhoz Mader 3775, Curitiba 81350-010, PR, Brazil
[c] Plataforma de Espectrometria de Massas-RPT02H, Instituto Carlos Chagas-Fiocruz, Rua Prof. Algacyr Munhoz Mader 3775, Curitiba 81350-010, PR, Brazil

ARTICLE INFO

Keywords:
Lutzomyia longipalpis
Leishmania infantum chagasi
Exosomes
Virulence factors

ABSTRACT

Leishmania infantum chagasi is the primary etiological agent of visceral leishmaniasis in Latin America, a lethal disease that afflicts hundreds of thousands of people worldwide every year. Previous studies have shown that the parasite releases microvesicles known as exosomes, which prolong and exacerbate infection in the vertebrate vector. However, little is known of their role in the insect vector, the sand fly *Lutzomyia longipalpis*. Exosomes were isolated from cultured *L. i. chagasi* in logarithmic (procyclic) (LOG) and stationary phase (metacyclic-like) (STAT) growth stages, which are the parasite stages found in the vector, and submitted to proteomic analysis. Our studies showed that exosomes from LOG and STAT *L. i. chagasi* display discrete protein profiles. The presence of approximately 50 known virulence factors was detected, including molecules for immunomodulation and evasion (GP63, EF1α, Oligopeptidase), increased pathogenicity (Casein kinase, KMP-11, Cysteine Peptidase and BiP) and parasite protection (Peroxidoxin). Additionally, the majority of ontological terms were associated with both exosome phases, and no substantial ontological enrichment was observed associated with any of the two exosomal stages. We demonstrated that LOG exosomes show a marked increase in protein number and abundance, including many virulence factors, compared to STAT *L. i. chagasi* exosomes.

Significance: The knowledge of the role of *Leishmania* exosomes on leishmaniasis opened up a new world of potential and complexity regarding our understanding of the disease. In Brazil the majority of visceral leishmaniasis cases are caused by the parasite *Leishmania infantum chagasi* and transmitted by the vector *Lutzomyia longipalpis*. While *Leishmania* exosomes were found to play an active role in the mammalian host, little is understood about their effects on the sand fly, or how they might impact on the insect infection by the parasite. For this reason, we isolated exosomes from two developmental stages of *L. i. chagasi* that occur within the insect with a view to identifying and describing the alterations they undergo. We have identified many hundreds of proteins within both exosome phases and have developed a structure by which to examine potential candidates. Our findings regarding the composition of the exosome proteome raise many questions regarding their function and provide compelling evidence that exosomes play an active role in the parasite's development within the sand fly.

1. Introduction

Leishmaniases are caused by protozoan parasites belonging to the genus *Leishmania* [1], which cause multiple clinical forms of disease, including cutaneous leishmaniasis (CL), a benign but frequently disfiguring skin condition which has a tendency towards spontaneous resolution, and visceral leishmaniasis (VL), a potentially fatal condition that results from the dissemination of *Leishmania* in macrophage-rich tissues [2].

Based on estimates, there are approximately 200 to 400 thousand new VL cases per year [3,4,5]. Visceral leishmaniasis has a worldwide distribution in 76 countries and endemicity in 12 countries of the Americas [3]. Reported leishmaniasis case figures are widely acknowledged to represent gross underestimates of the true disease burden, and studies that measure the degree of underreporting are rare [4]. The most recent Pan American Health Organization (PAHO) study has described worsening conditions for the spread of these diseases with showing the highest VL mortality rate (7.9%). Brazil has 96% of all

* Corresponding author.
E-mail addresses: dmfiocruz@gmail.com (D.M. Forrest), michel.batista@fiocruz.br (M. Batista), fabricio.marchini@fiocruz.br (F.K. Marchini), tempone@ioc.fioruz.br (A.J. Tempone), ytraub@ioc.fiocruz.br (Y.M. Traub-Cseko).

https://doi.org/10.1016/j.jprot.2020.103902
Received 16 December 2019; Received in revised form 18 April 2020; Accepted 8 July 2020
Available online 14 July 2020

American VL cases, with the most at-risk demographics being children [6]. *Leishmania infantum chagasi* is the etiological agent for zoonotic VL in Central and South America and its primary vector in the New World is *Lutzomyia longipalpis* [7].

After the vertebrate host receives an infective bite, metacyclic promastigotes are phagocytised by macrophages and neutrophils [8]. Inside the phagolysosomal lumen, promastigotes develop into amastigote forms, which replicate by binary fission, leading to the eventual disruption of the host cells. Amastigotes are thus liberated into the extracellular milieu and, in their turn, infect surrounding macrophages, which will be picked up by a biting vector.

Leishmania development in the hematophagous sand fly vector occurs exclusively in the digestive tract of the insect. Amastigotes ingested during a bloodmeal develop into procyclic promastigotes. After the peritrophic matrix disintegrates, promastigotes attach themselves to the midgut wall [9,10] to avoid being expelled with the digested material and later develop into infective metacyclic forms, which migrate to the anterior parts of the digestive tract and infect new hosts through the insect bite, thus closing the cycle.

One of the methods by which eukaryotic pathogens spread effector molecules is the secretion of membrane vesicles which originate from the plasma membrane or intracellular compartments. The exosome is one such type of vesicle [11]. Exosomes are small 30-100 nm vesicles, containing an array of biomolecules, including proteins as well as carbohydrates, lipids and nucleic acids [12]. The process of exosome biogenesis within the endosomal lumen is characterized by an inward budding of the endosomal limiting membrane. This produces exosomes with an intracellular cytosolic profile and an inverted endosomal membrane profile [13,14,15].

Silverman and colleagues were the first to describe *Leishmania* exosomes while studying the *Leishmania donovani* secretome [16]. This group later went on to refine a description of an exosome-based secretion pathway for *Leishmania* and ascribe to it the function of protein-transport and communication [17]. Later studies have aimed to elucidate the primary activities of these extracellular vesicles (EVs) and other non-vesicular extracellular material in the context of mammalian infection, finding, among other things, their propensity to attract dendritic cells upon infection, potentiate infection [18,19], suppress immune effectors such as TNF-α and IL-8 [20], LPS [18] and IL-1β [21], and suppress iNKT cell expansion [22]. These studies have helped construct a character profile of exosomes as agents of pro-virulence acting primarily through immunomodulatory mechanisms.

Only one study to date has investigated *Leishmania* exosomes in the sand fly [23], demonstrating active exosome secretion within the midgut, and egestion during sand fly feeding, as well as their subsequent pro-virulence effect in the murine model.

Leishmania must traverse different hosts and undergo several developmental changes in response to its environment. In the sand fly host parasites entering the midgut must survive digestion, migrate to the anterior midgut and ready themselves for egestion into the vertebrate host. Exosomes have been widely demonstrated to immunomodulate the mammalian host to favour the *Leishmania* parasite [24]. We have shown sophisticated immune responses of *L. longipalpis* related to various challenges, including modulation of negative immune regulators [25] and defensin [26] in response to bacteria and *Leishmania*; the presence of active Toll and IMD immune pathways [27], and the presence of a non-specific dsRNA-mediated antiviral response [28]. We are currently interested in establishing a role for *Leishmania* exosomes in these responses. *Leishmania* appears to secrete exosomes throughout all stages inside the vector. As such this begs the question of whether these exosomes reflect developmental changes of the parasite, a defence against host responses or an offensive weapon for subversion of host processes. It is therefore of interest to know whether the composition of these vesicles is being modified, what such modifications might entail and how they might relate to the current models of parasite-host interaction.

As a first step towards this goal this study aimed to describe the proteomic profiles of exosomes isolated from two growth phases of *L. i. chagasi* corresponding to vector early midgut-establishing logarithmic (LOG) and later anterior gut-establishing stationary (STAT) parasites using mass spectrometry (MS/MS). Cultured parasites were used due to obvious difficulties of obtaining exosomes from *Leishmania* at different stages of development directly from insects. A preponderance of protein identities and abundance was found in LOG compared to STAT exosomes, as well as a highly skewed distribution of protein members and a plethora of previously characterized virulence factors in both groups. As such, exosomes isolated from both phases of *L. infantum chagasi* represent caches of pro-virulence factors that may be involved in parasite establishment within the sand fly, or, for late infective stages, with a function in mammalian infection.

2. Materials & methods

2.1. Parasite culture

Exosomes were isolated from *L. i. chagasi* (MHOM/BR/1974/PP75) obtained from the *Leishmania* collection of Instituto Oswaldo Cruz, maintained at 26 °C in 199 Medium (Gibco-Life Technologies) supplemented with 10% foetal bovine serum (FBS) (Econolab), HEPES 40 Mm, adenine 100 μM, hemin 2,5 μg/mL and 1% antibiotics (penicillin 100 U/mL and streptomycin 100 mg/mL -Sigma). Passages were performed every 2–5 days. Growth curves (Fig. S1) were used to establish logarithmic and stationary phase parasites from which exosomes would ultimately be isolated.

2.2. Exosome collection

Leishmania cultures were seeded at a density of 1×10^6 parasites/mL culture and allowed to grow uninterrupted for 3 days to produce logarithmically growing cultures. After 3 days parasites were pelleted by centrifugation at 1500 ×*g* for 10 min at 4 °C and washed 3 times with un-supplemented M199. Parasites were replaced into new M199 media supplemented with 10 % Tryptose Phosphate Broth (TPB [Sigma Life Sciences T8159]) instead of FBS and grown for 24 h at 26 °C, as the latter contains exosomes. After this period exosomes were recovered by differential centrifugation using 300 ×*g* for 10 min to remove live parasites, 2000 ×g for 10 min to remove dead parasites and large cellular debris, 10,000 ×g for 30 min to further remove cellular debris and large vesicles and finally ultracentrifugation at 100,000 ×*g* for 60 min to pellet exosomes. Exosome pellets were resuspended in ice-cold PBS 1× and submitted to a second washing round of ultracentrifugation. The re-pelleted exosomes were then resuspended in PBS 1× to a final volume between 80 μL and 150 μL before being submitted to quantification using the Pierce 660 nm colorimetric assay.

Stationary phase parasites that had grown for 6 days uninterrupted were pelleted, washed and resuspended as with logarithmic phase parasites. However instead of new M199, the original culture medium was submitted to centrifugation in order to remove accumulated exosomes before reintroducing parasites for a further 24 h period. Exosomes were then recovered from stationary phase parasites exactly as with logarithmic parasites. Three biological replicate exosome samples were recovered from both LOG and STAT cultures.

2.3. Exosomal protein quantification

To quantify exosome proteins the Pierce 600 nm colorimetric assay was performed as follows: 4 μL of exosomes in PBS 1× was added to 4 μL of a 0.6 % TX-100 solution in order to disrupt exosome membranes and release the proteins into solution. BSA was used to establish a standard curve of protein concentration between 50 and 2000 ng/μL against which serial dilutions of exosome protein were assessed using a Nanodrop 8000 spectrophotometer.

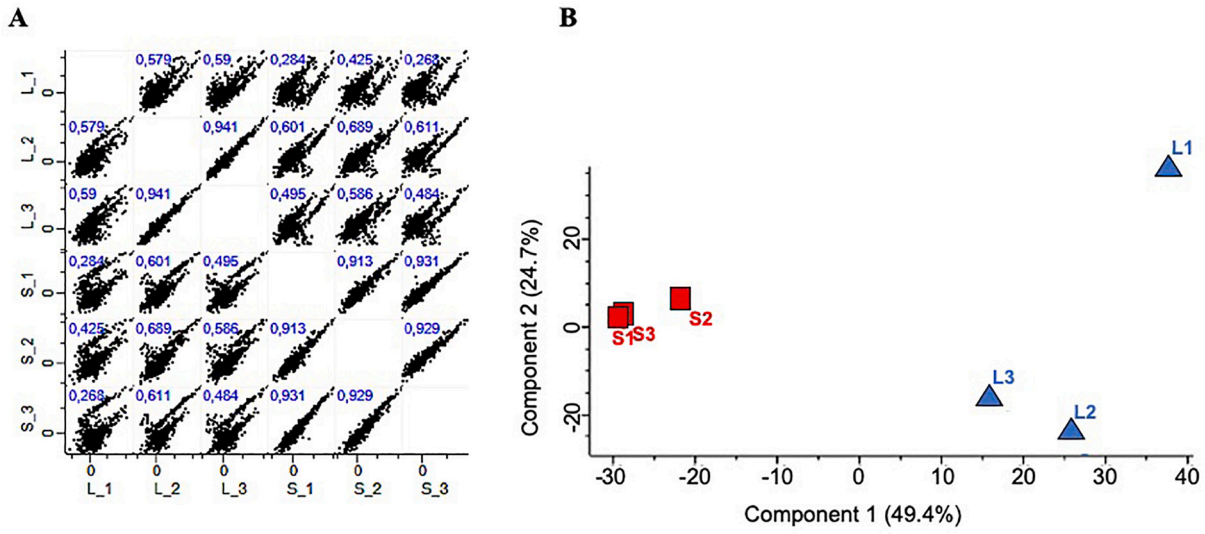

Fig. 1. Pearson Correlation and PCA.
Pearson Correlation plots (1A) showing the inter-sample correlation of LOG and STAT exosomes. R^2-values obtained from between-group sample comparisons were low, ranging from 0.2–0.7, suggesting that LOG and STAT groups exhibit statistically divergent profiles. R^2-values obtained from within-group sample comparisons were generally high > 0.9 (1 being a perfect correlation), suggesting good replicability of sample isolation. The only exception to this was L1 divergence from its sister replicates. Secondary comparison using Principal Component Analysis (1B) was used to investigate L1 clustering with its sister replicates. This analysis shows group-specific clustering of LOG (L) (blue) and STAT (S) (red) in the first component. However, in the second component sample L1 diverges substantially from its sister replicates and so was removed from further analysis in this study. (For interpretation of the references to colour in this figure legend, the reader is referred to the web version of this article.)

2.4. Proteomic analysis

Ten μg of each sample (LOG and STAT) was run on a 12% SDS-PAGE gel, the entire lane of each sample was excised, and triplicate samples were submitted for proteomic analysis at the mass spectrometry facility RPT02H at Instituto Carlos Chagas, Fiocruz in Curitiba, Paraná.

The protein samples were subjected to in-gel digestion. First, proteins were reduced in 10 mM DTT at 56 °C for 1 h and alkylated in 55 mM iodacetamide at 25 °C for 45 min protected from light. After that, gel pieces were incubated with 12.5 ng/μl trypsin (Promega) in 50 mM ammonium bicarbonate at 37 °C for 18 h. Then, peptides were extracted from the gel matrix, followed by desalting in a homemade C18 stage-tips. The peptides were analysed by LC-MS/MS in triplicate in an EASY nLC 1000 coupled to a LTQ Orbitrap XL ETD mass spectrometer (Thermo Scientific) equipped with a nanoelectrospray ion source (Phoenix S&T). The peptides were loaded onto a 30 cm fused silica capillary (75 μm i.d.) in-house packed with 1.9 μm C18 reversed phase (Dr. Maisch). The peptides were eluted from the capillary with a linear acetonitrile gradient (5–40 % (*v*/v) / 120 min) in 0.1 % (v/v) formic acid and 5 % (v/v) DMSO at a flow rate of 250 nL/min. The spray voltage used was 2.7 kV, spray current 100 μA, capillary voltage 35 V, tube lens 100 V, and tube transfer 175 °C. Full-scan mass spectra were acquired in the orbitrap within a *m/z* window ranging from 300 to 2000, resolution of 60,000 at 400 m/z and AGC target of 10^6. The option lock mass was enabled at 401.922718 m/z to improve mass accuracy. The MS/MS was carried out in the linear ion trap, where the 10 most intense precursor ions from each full scan were isolated at an AGC target of 3×10^4 and fragmented by CID. The precursor ions were dynamically excluded for 90 s.

2.5. In Silico analysis

First-stage manipulation of Mass Spectrometry data was performed through MaxQuant algorithm version 1.4.1.2. Default parameters of the software were used for all analysis steps, unless stated otherwise. The UniProt protein database was used to provide the most comprehensive ID coverage and prediction for the peptides in each sample. Downstream statistical manipulation and analysis of peptide ID lists was performed with Perseus (v1.5.5.3) using standard software parameters. Distribution of peptide counts was normalised through log-transformation and width adjustment, to produce data sets from which reliable statistical analyses could be applied. The dataset was then evaluated using Pearson Correlation, Principal Component Analysis (PCA), and two-sample *t*-tests (FDR = 0.05 in all cases) to produce functional statistical comparisons of the exosome groups.

2.6. Protein member analysis

Due to the high number of identified protein species, we sought to create a structure that would help to order these proteins in terms of potential importance. We chose broad categories into which proteins of interest might fall: abundant proteins – those with Label-Free Quantification (LFQ) values that placed them within the top 50 most abundant proteins of at least one exosome group; modulated proteins – those proteins shared between LOG and STAT phase but whose LFQ values fluctuate significantly, as identified by *t*-test, from one group to the other; and finally virulence factors – those proteins identified within previous literature that exhibit either a direct or indirect positive influence upon parasite virulence in any host system and in any *Leishmania* spp. Proteins occupying all three categories would be of most interest, followed by those occupying two of the three categories, and lastly, those represented within only one category. In this way we produced a hierarchy of potential interest populated at each level by various numbers of proteins.

2.7. Meta-data analysis

Protein IDs were submitted to the TriTrypDB (http://tritrypdb.org/tritrypdb/) Gene Onthology (GO) analysis database. Only ontological terms significantly associated with the protein members submitted were included in this analysis. Only proteins found in all replicates of at least one growth phase group were included in the analysis.

2.8. STRING network analysis

We performed an interaction analysis of the 50 most abundant *L. infantum* LOG and STAT phase exosomal proteins by using the Search Tool for the Retrieval of Interacting Genes/Proteins (STRING) database V 11 at http://string.embl.de/.

3. Results

3.1. Pearson correlation and PCA analysis

The statistical correlation of Log_2 intensity values between all three replicates from both phases was analysed using Pearson Correlation (Fig. 1A). Scatter plots demonstrated a high degree of within-group correlation ($R^2 > 0.9$), while between-group plots gave R^2 values of < 0.6. However, one logarithmic sample diverged substantially from its sister replicates. To substantiate this observation, the clustering of exosome replicates was analysed using PCA (Fig. 1B). Results showed that LOG and STAT exosome groups clustered separately along the 1st component, indicating that the groups show statistical variance from one another. This variance was reduced along the 2nd component; however the same logarithmic replicate remained disparate within its group and was therefore removed from further analysis. This analysis demonstrated that LOG and STAT exosomes possess statistically distinct Log_2 intensity distributions.

3.2. Protein profile of LOG vs STAT exosomes

A total of 1037 proteins were identified. When considering proteins that were present in all replicates of at least one phase this number dropped to 647, with 615 and 354 proteins in LOG and STAT phases respectively (Table S1). Of these, 323 were shared between both phases (Fig. 2). Within this shared group 83 were significantly positively modulated in LOG compared to STAT, and 16 significantly positively modulated in STAT compared to LOG. There were 85 proteins found exclusively in LOG replicates, and 17 proteins found exclusively in STAT replicates. All other proteins were present in at least 1 replicate of both phases.

3.3. Exosomal origin of the proteins

In order to confirm the exosomal origin of the samples used in this study and establish the successful isolation of an exosomal fraction of *Leishmania*-derived extracellular vesicles, the protein ID database generated from proteomic *in silico* analysis was mapped against the ExoCarta database (http://exocarta.org/exosome_markers_new), which lists the top 100 exosomal protein markers most often found in exosome samples. Of the 53 markers that had homologues in *Leishmania infantum,* 50 were identified in our recovered samples (Table S2) Additionally, we used PrediSi online tool (http://www.predisi.de/) to investigate the presence of signal peptides in our identified proteins. As expected, of the 1037 proteins identified in our exosome samples, 954 (91.9%) showed no signal peptide. Of the 615 proteins present in all LOG replicate samples 564 (91.7%) showed no signal peptide. Of the 354 proteins present in all STAT replicate samples 323 (91.2%) showed no signal peptide (Table S1). These two analyses suggest the vast majority of our proteins are secreted by non-classical pathway and indicate that we succeeded in recovering *bona fide* exosomes.

3.4. Peptide intensity distributions

We found that protein intensities (unlogged) exhibited a highly skewed distribution (Fig. 3A), where approximately 80 % of total measured protein intensities (averaged between replicates) was accounted for by only 20 % of protein members. Likewise, the 4 most abundant proteins (less than 1 % of protein members) in each phase were responsible for ~20 % of the total measured intensities (GP63, EF1a, HSP70 and HSP83 in LOG and EF1α, Beta-tubulin, GP63 and HSP70 in STAT). Log2 scale distributions showed both conditions produced normal intensity distributions (Fig. 3B). Additionally, when average protein LFQ values were compared, we found that the vast majority of proteins showed higher abundance in LOG exosomes (Fig. 3C, D).

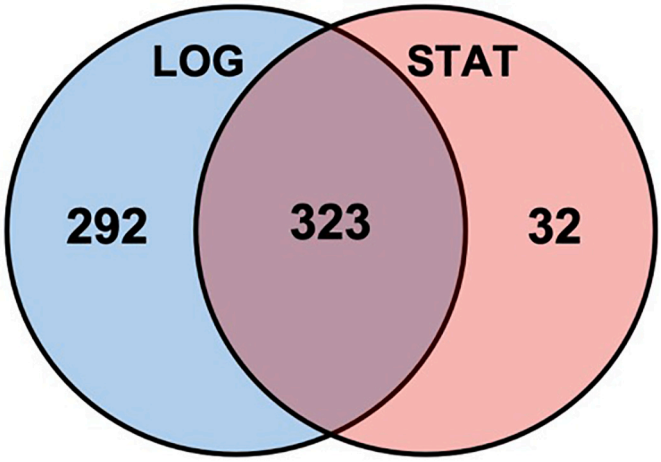

Fig. 2. LOG *vs* STAT protein profile.
Venn diagram showing the number of proteins identified in LOG and STAT *Leishmania* exosomes. Of the 1037 proteins identified, this study considered only the 647 that were present in all replicates of at least 1 exosome group; 323 of these were present in all replicates of both groups, while 292 were identified only in all LOG replicates (LOG) (blue), and 32 only in all STAT replicates (STAT) (red). (For interpretation of the references to colour in this figure legend, the reader is referred to the web version of this article.)

3.5. Protein member analysis

The 50 most abundant proteins accounted for ~66 % and 69 % of total measured intensities in LOG and STAT groups respectively. Thirty proteins identified as among the most abundant (within the top 50) in LOG exosomes were also present in the top 50 of STAT exosomes comprising 56 % (LOG) and 49 % (STAT) of total intensities. A total of 99 proteins were found to be modulated from LOG to STAT phase, comprising 29.3 % and 28.8 % of LOG and STAT total intensities respectively. Of these, 83 were positively modulated in LOG, comprising 29.2 % and 16.3 % of LOG and STAT total intensities respectively, and the remaining 16 positively modulated in STAT, comprising 0.14 % and 12.5 % of LOG and STAT total intensities respectively. Of the 80 or so virulence factor candidates identified from previous literature, 51 were present in our exosomes; 51 in LOG and 48 in STAT accounting for ~42 % and 32 % of total measured intensities respectively (Table S3). Proteins of interest falling into these three categories collectively account for ~76 % and 79 % of total intensities in LOG and STAT exosomes respectively. Regarding proteins that occupy only one category, 32 were abundant-only (Table S4), 69 were modulated-only (Table S5) and 23 were virulent-only (Table S6). Regarding proteins that occupy two categories, 16 were abundant and modulated (Table 1), 15 were abundant virulence factors (Table 2) and 7 were modulated virulence factors (Table 3). Finally, 6 proteins were identified as virulence factors which were both abundant and modulated (Table 4).

3.6. Meta-analysis – GO term and pathway enrichment

There were 313/615 LOG proteins and 200/354 STAT proteins to which GO terms were significantly associated and 179 of these were common between the two groups (Table S7). There were 24 and 16 terms significantly associated with LOG and STAT proteins respectively.

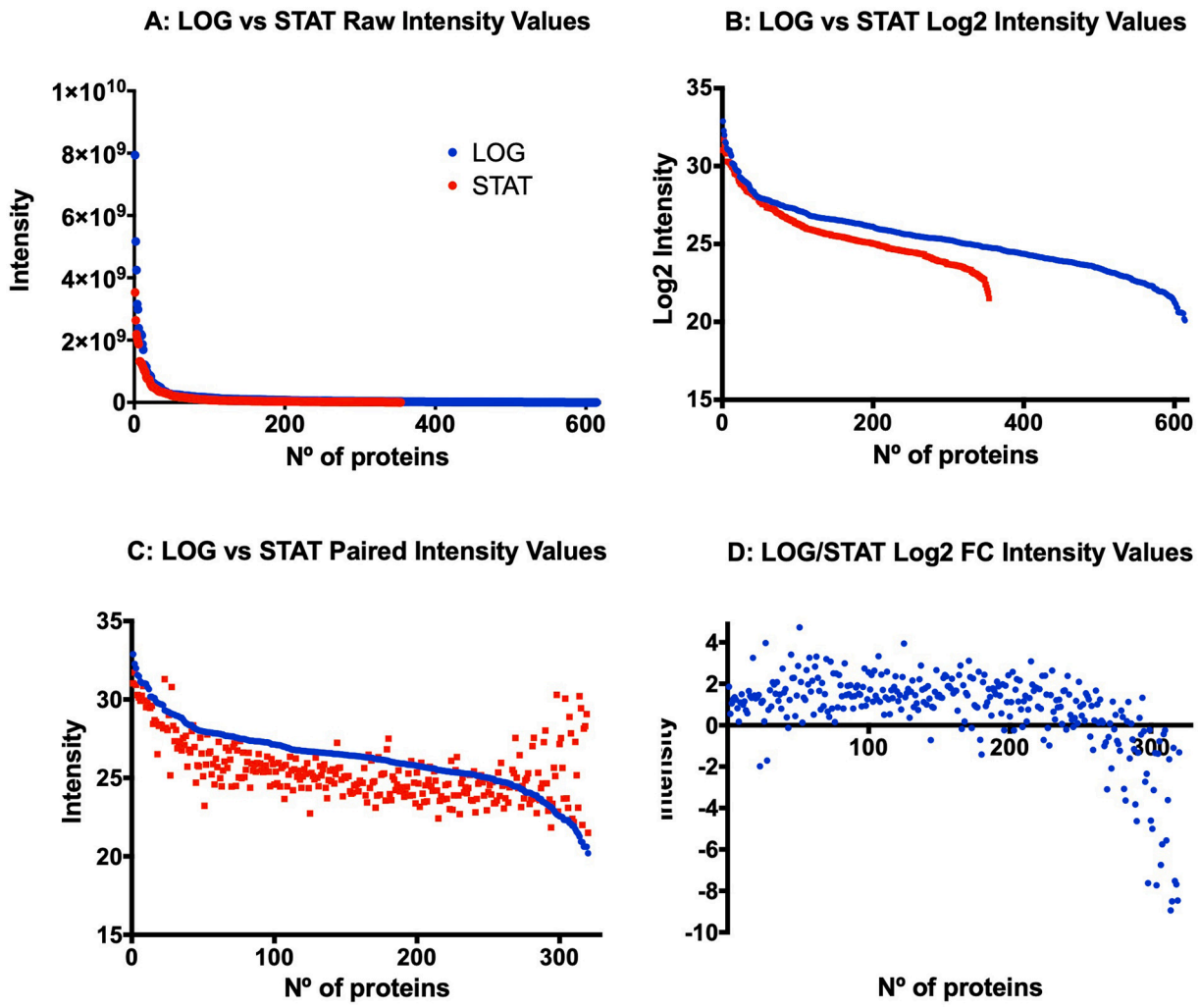

Fig. 3. Protein LFQ Intensity Distributions.
(3A): Rank-ordered, unlogged LFQ values for all proteins identified in all replicates of LOG and STAT group. (3B): Rank-ordered, Log2 LFQ values showing a normal distribution is present in both groups. (3C): X-axis-paired Log2 LFQ values of 323 shared proteins where LOG group is rank-ordered. (3D): Fold change Log2 LFQ values LOG/STAT, where Log2 intensity values derived from STAT are standardized at a reference value of 0. (LOG = blue and STAT = red). (For interpretation of the references to colour in this figure legend, the reader is referred to the web version of this article.)

Thirteen of these terms were shared between groups while 11 and 3 were specific to LOG and STAT respectively. Sixty-seven and 45 proteins from LOG and STAT groups respectively were associated with enriched pathways. Both GO analysis and pathway enrichment analysis showed a substantial overlap in the terms significantly associated to LOG and STAT exosomes. When considering the numbers of proteins associated with each term, however, we found that the STAT group showed a real increase in protein members only in 3/31 terms, whereas LOG group showed a real increase in 35/40 terms. Most significant terms showed a pronounced drop in protein number from LOG to STAT, and several pathway enrichment terms contained protein members for LOG alone. Additionally, in the 3 cases where STAT group showed an increase in term-associated protein members, this was not due to the presence of STAT-specific proteins (Fig. 4).

3.7. STRING network analysis

The Prevised Protein Interaction (PPI) enrichment *p*-value was 1.18e-07 for LOG and 4.14e-11 for STAT, indicating that secreted proteins have more relations among themselves than what would be expected for a random set of proteins of similar size drawn from the genome Fig. 5. Protein functional enrichment analysis from both groups identified enhanced interactions related to specific biological functions. In the LOG phase the STRING algorithm identified 7 Kyoto Encyclopedia of Gene and Genomes (KEGG) pathways significantly enriched (Table S8), with emphasis on the Glycolysis/Gluconeogenesis pathway (lif00010) showing a False Rate Discovery (FDR) of 9.1e-05. The same analysis showed that associations among the STAT phase exosomal proteins revealed two Biological processes (GO) and two KEGG pathways significantly enhanced: peptide metabolic process GO:0006518 and translation GO:0006412; and the ribosome (lif03010) and endocytosis (lif04144) pathways.

4. Discussion

Leishmania have been found to release exosomes throughout all phases of its lifecycle, both in the mammal [19] and the vector host [23]. As mentioned before, while a lot is known about exosomes' interaction with the mammalian host in leishmaniasis and other vector borne infectious diseases [12], little is known on how these secreted vesicles might impact parasite development inside the vector host. This study investigated the protein composition of *L. infantum*-derived exosomes from both logarithmic and stationary-phase parasites grown in culture, which mimic the stages found in the insect, in order to examine whether these microvesicles reflect changes in the parasite or its interaction with the insect host.

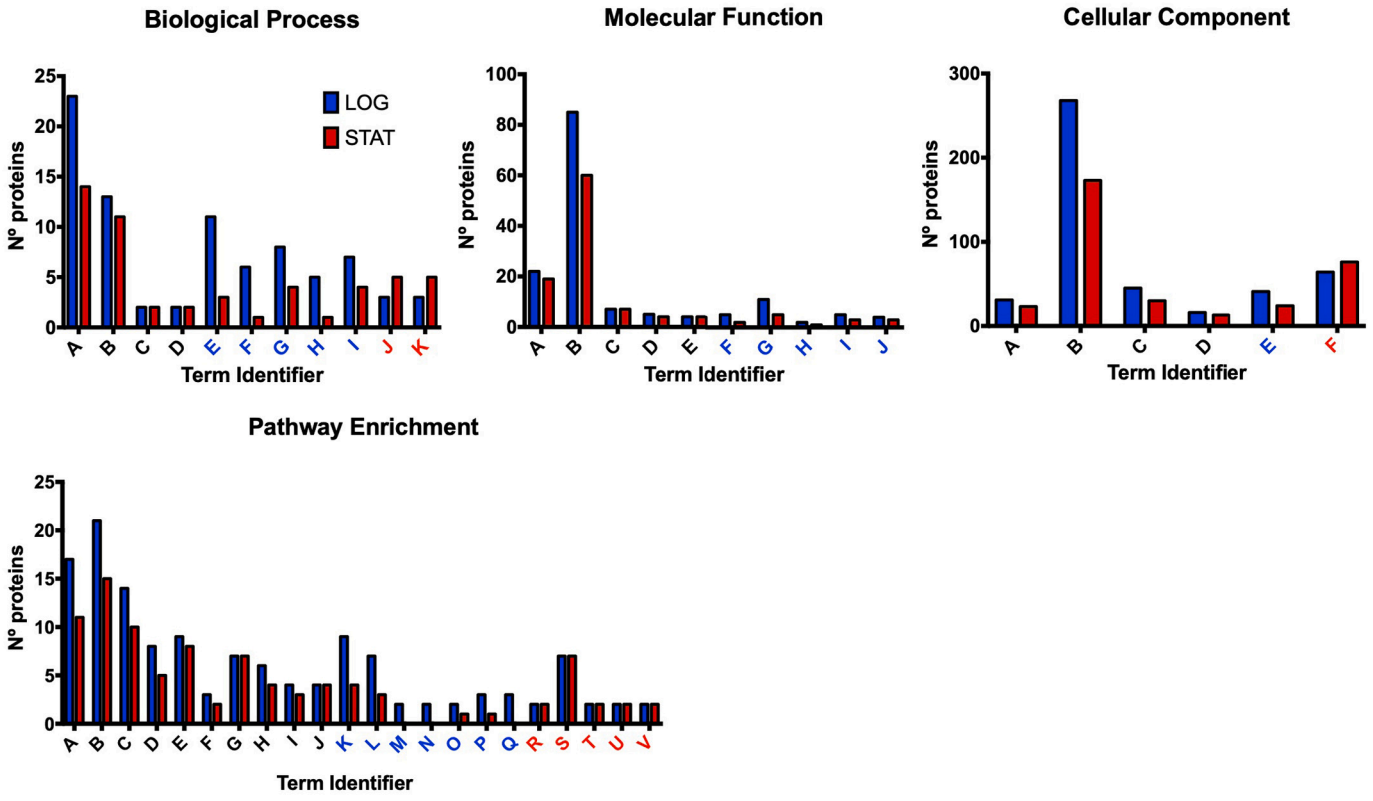

Fig. 4. Meta-analysis.
The GO and Pathway Enrichment terms associated significantly with LOG and/or STAT protein group. (4A): Biological Process GO category (A = GO:0044281 small molecule metabolic process, B = GO:0009056 catabolic process, C = GO:0000902 cell morphogenesis, D = GO:0048856 anatomical structure development, E = GO:0030705 cytoskeleton-dependent intracellular transport, F = GO:0006520 cellular amino acid metabolic process, G = GO:0006412 translation, H = GO:0000278 mitotic cell cycle, I = GO:0007010 cytoskeleton organization, J = GO:0034655 nucleobase-containing compound catabolic process, K = GO:0006091 generation of precursor metabolites and energy). (4B), Molecular function GO category (A = GO:0043167 ion binding, B = GO:0003674 molecular function, C = GO:0008233 peptidase activity, D = GO:0016829 lyase activity, E = GO:0008092 cytoskeletal protein binding, F = GO:0016874 ligase activity, G = GO:0016887 ATPase activity, H = GO:0016798 hydrolase activity, acting on glycosyl bonds, I = GO:0016853 isomerase activity, J = GO:0008135 translation factor activity, RNA binding). (4C) Cellular Component GO category (A = GO:0005829 cytosol, B = GO:0005737 cytoplasm, C = GO:0005654 nucleoplasm, D = GO:0005777 peroxisome, E = GO:0032991 protein-containing complex, F = GO:0005634 nucleus). (4D) Enriched Pathway category (A = TRNA-CHARGING-PWY tRNA charging pathway, B = PWY3IU-99 superpathway of central carbon metabolism, C = PWY3IU-61 superpathway of glycolysis, pyruvate dehydrogenase and TCA cycle, D = ANARESP1-PWY respiration (anaerobic), E = GLUCONEO-PWY gluconeogenesis I, F = PWY3IU-623 GDP-mannose biosynthesis, G = GLYCOLYSIS glycolysis I, H = PWY3IU-1026 methionine salvage pathway, I = PENTOSE-P-PWY pentose phosphate pathway, J = PWY-5143 fatty acid activation, K = PWY3IU-445 purine nucleotide metabolism (phosphotransfer and nucleotide modification), L = TCA TCA cycle, M = PWY3IU-6 glutamate degradation, N = OXIDATIVEPENT-PWY pentose phosphate pathway (oxidative branch), O = PWY3IU-26 mannogen metabolism, P = SUCSYN-PWY sucrose biosynthesis, Q = PWY-4041 & gamma;-glutamyl cycle, R = CYSTSYN-PWY cysteine biosynthesis I, S = PWY3IU-1054 fatty acid β-oxidation, T = PWY-801 homocysteine and cysteine interconversion, U = PWY-4081 glutathione redox reactions I, V = HOMOCYSDEGR-PWY cysteine biosynthesis/homocysteine degradation). Black letters = terms significant in both LOG and STAT group. Blue letters = terms significant only in LOG group. Red letters = terms significant only in STAT group. (For interpretation of the references to colour in this figure legend, the reader is referred to the web version of this article.)

Our results show that both phases of exosomes exhibit statistically discrete phenotypes, suggesting roles for exosomes that are stage specific. While there is no technical reason for LOG replicate 1 to have deviated statistically from its sister replicates, it was also the first sample produced in the project and may have been subject to human error. Additionally, variance was more pronounced in the LOG group as a whole compared to the STAT group, which may simply reflect the higher metabolic activity of the LOG group parasites. The analysis showed a highly skewed distribution of proteins regarding their abundance in exosomes, where a handful of protein species represented the majority of the total protein. This may indicate that most of the functionality of these exosomes is carried out by a small number of protein members.

Of most interest were the 6 protein species that were abundant, modulated virulence factors (Table 4). These included GP63, EF1α, Actin, Calpain-like Cysteine Peptidase, Carboxypeptidase and S-adenosylmethionine Synthase. All of these proteins were positively modulated in LOG exosomes compared to STAT exosomes and the last three are abundant only in the LOG phase. While accounting for less than 1 % of the identified protein species in this experiment, together they account for ~17 % and 11 % of total protein in LOG and STAT exosomes respectively. The fact that both phases share such proteins and in such abundance suggests that there may be a conserved functionality between phases. Three of these candidates stood out in particular; GP63, EF1α and Cysteine Protease. GP63 is the most abundant surface glycoprotein of *Leishmania spp.* [29] and thought to be the primary virulence factor of this parasite. In the vertebrate host it has been shown to be involved in a myriad of processes from the moment of encountering host cells, through adhesion [30], internalization [31], survival [32,33] and modification [34] of the host system. Of particular interest in the last decade has been the indirect effects of GP63's activation of the phosphatase negative regulators such as protein-tyrosine-phosphatase SHP-1 and the consequent effect they may have on immune effectors such as MAPK [35,36,37]. GP63 has been shown to defend the parasite against antimicrobial peptides *in vitro* [38] and it has also been implicated in parasite attachment to the fly midgut [39].

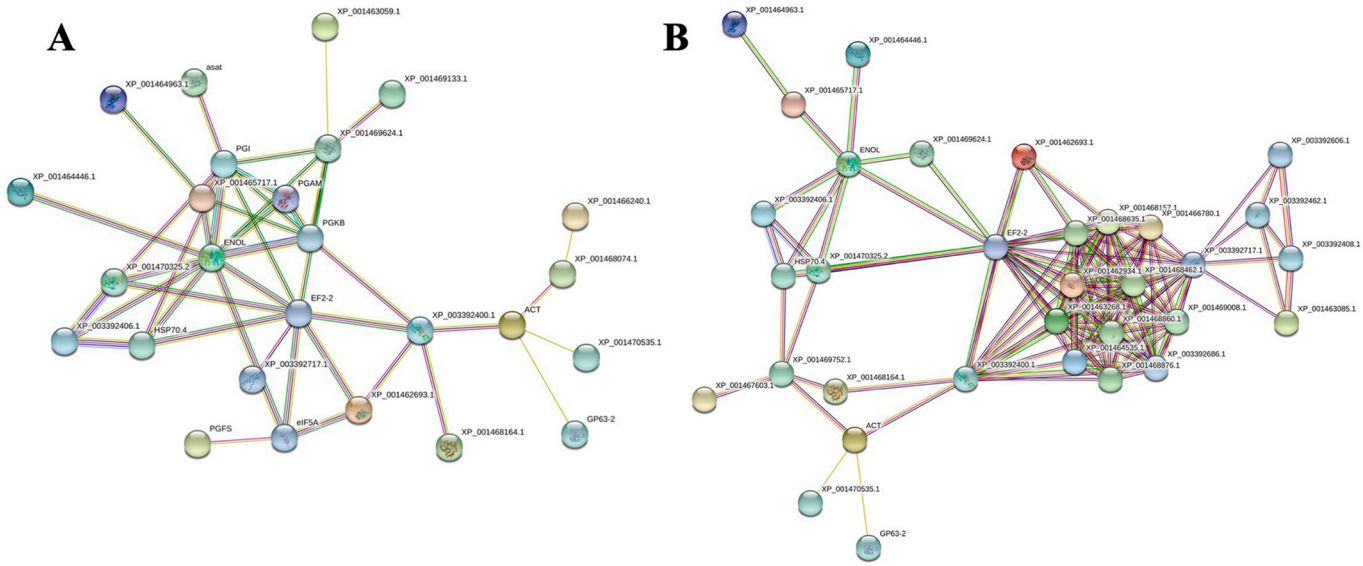

Fig. 5. STRING Interaction network of the 50 most abundant proteins in LOG (A) and STAT (B) phase exosomes. Proteins without connections were excluded, leaving only those connected.

There is much common ground between the mammalian immune pathways previously studied and those of sand flies (reviewed in [40]). As such GP63 represents a primary candidate in the examination of parasite-sand fly interactions.

EF1α was previously identified in *L. infantum* exosomes released *in vivo* within the sand fly midgut [23]. Most interesting to this current study is EF1α interactions with host phosphatases, particularly SHP-1 [41]. While the consequences of this interaction are still unclear [42], the immune implications are intriguing as SHP-1 is a negative regulator of both the Toll and JAK-STAT immune pathways. Indeed, iNOS expression response to IFN-y is attenuated in RAW267.4 mouse cells pretreated with purified *L. donovani* EF1α [41]. As such this protein may be exerting a similar immunosuppressive effect within the sand fly.

Calpain-like cysteine peptidase (CP) has previously been detected in both the exoproteome [43] and sand fly stage *in vivo* exosomes [44] of *L. infantum* and appears to be present in both promastigote and amastigote phases of the parasite [14]. Its role in the vertebrate host appears to be in the degradation of key signaling molecules such as inhibitory subunit of nuclear factor Kappa B-alpha (IkB-a), IkB-b and nuclear factor kappa B (NF-kB) in macrophages, and perhaps inhibiting LPS-mediated IL-12 production in macrophages [45]. Curiously, our exosomes showed a 3-fold decrease from LOG to STAT in the abundance of this CP.

Contrary to expectations, we found that the proportion of protein in each phase which was significantly comprised of modulated members, actually remained quite constant (~30 %). This was a result of the skewed intensity distributions once again, where 16 proteins comprising 0.14 % of LOG intensities increased to 12.5 % in STAT. These were mostly ribosomal subunit proteins. Similarly, the 83 proteins positively modulated in LOG, representing ~30 % of total protein intensities dropped to 16 % in STAT. Since none of the proteins positively modulated in STAT were known virulence factors but showed a positive increase contrary to the general fall in protein abundance from LOG to STAT, these few ribosomal proteins may serve an important function specific to STAT-phase exosomes. Alternatively, if exosomes act as a method of protein disposal, they may reflect metabolic changes in the STAT-phase parasite.

We found in both exosome phases several hundred protein species that span a range of functional roles. However, our meta-analysis indicated that the most notable change from LOG to STAT phase

Table 1
Abundant, modulated proteins: Proteins abundant in at least one exosome phase, modulated between exosome phases but not previously associated with parasite virulence.

Abundant + Modulated				Average LFQ (Log2)		LOG/STAT
	Uniprot ID	Protein Annotation	Peptide #	LOG	STAT	Log2 LFQ Ratio
LOG	A4IBL4	Putative cystathione gamma lyase	9	28.4	26.8	1.6
	E9AGE1	Glucose-6-phosphate isomerase	16	28.0	26.6	1.4
	Q2PD92	Aspartate aminotransferase	18	28.1	25.8	2.3
	A4HRH5	Putative long-chain-fatty-acid-CoA ligase	17	28.0	25.7	2.3
	A4HXG5	Putative META domain containing protein	17	29.1	25.2	4.0
	A4I8K5	Myosin XXI	24	28.0	25.1	2.9
	A4I8N8	Uncharacterized protein	13	28.1	24.7	3.4
STAT	A4IDD3	Clathrin heavy chain	41	22.7	30.3	−7.6
	E9AHI5	Putative ribosomal protein L1a	13	21.3	30.2	−8.9
	A4HW98	Histone H4	9	22.3	30.1	−7.7
	A4I7Q4	60S ribosomal protein L18a	7	20.9	29.4	−8.5
	A4HS71	Putative 60S ribosomal protein L10	8	20.6	29.1	−8.5
	E9AGQ7	Histone H2B	5	22.1	28.9	−6.7
	A4IB89	Putative 60S Ribosomal protein L36	3	20.6	28.3	−7.7
	A4HWU4	Putative 60S ribosomal protein L21	5	20.6	28.1	−7.5
	A4I7K4	Putative ATP-dependent RNA helicase	12	23.4	28.0	−4.6

Table 2
Abundant virulence Factors: Proteins abundant in at least one exosome phase and previously associated with parasite virulence but were not modulated between exosome phases.

Abundant + Virulent				Average LFQ (Log2)		LOG/STAT
	Uniprot ID	Protein Annotation	Peptide #	LOG	STAT	Log2 LFQ Ratio
Shared	A4I412	Putative heat-shock protein hsp70	38	32.0	30.9	1.1
	E9AGJ8	Alpha tubulin	15	29.1	30.8	−1.7
	E9AHM9	Heat shock protein 83–1	40	31.6	30.3	1.3
	A4HYX4	Putative small myristoylated protein-1	6	31.1	30.2	0.8
	A4ICW8	Elongation factor 2	44	31.5	30.1	1.4
	A4HW62	Enolase	22	31.2	29.9	1.2
	A4ID05	Adenosylhomocysteinase	22	30.1	28.4	1.6
	A4I253	Heat shock protein 70-related protein	26	29.1	28.3	0.7
	A4HRK0	robable eukaryotic initiation factor 4A	20	29.6	28.2	1.5
	Q95NF5	Cytosolic peroxiredoxin	10	29.2	28.0	1.2
LOG	A4HW29	Putative calpain-like cysteine peptidase	6	28.9	26.9	2.0
	A4I1P9	Putative 2,4-dihydroxyhept-2-ene-1,7-dioic acid aldolase	7	28.4	26.6	1.8
	E9AHJ2	Putative paraflagellar rod protein 1D	17	28.4	25.7	2.7
STAT	A4IAU1	40S ribosomal protein S3a-2	9	21.5	28.8	−7.3
	A4IBB3	Kinetoplastid membrane protein-11	5	27.9	27.8	0.1

exosomes was the size of the protein profile rather than its functional character, with only 3 functional terms showing an increase (though small) in the number of protein members from LOG to STAT phase. This was particularly true regarding pathway enrichment, where terms associated only with STAT phase actually showed the same number of protein members as LOG. This is likely due to the smaller STAT dataset making statistical significance more probable than in LOG. Both exosome phases showed the largest majority of proteins localized to the cytosol and to a lesser extent the nucleus (Fig. 4C). The larger proportion of nucleus-localized proteins in STAT can be explained entirely by the presence of various 40S and 60S ribosomal subunit proteins. Similarly, the most populous terms were shared between groups, including small molecule metabolic process, catabolic process, and ion binding. LOG exosomes showed the greatest increase in Biological Process terms, including cellular amino acid metabolic process, translation, mitotic cell cycle, and cytoskeleton organization. Similarly, Pathway Enrichment terms also showed increases in LOG phase, including purine nucleotide metabolism, TCA cycle, glutamate degradation, pentose phosphate pathway, and mannogen metabolism. The enrichment of all of these terms might be explained by LOG phase parasites' mitotic and high metabolic activity whereas STAT phase parasites do not divide. This meta-analysis is a qualitative tool, assuming that all proteins are present in the same quantity within exosomes. Our demonstration of a severely skewed distribution means that this meta-analysis is limited in its ability to predict exosome functionality.

The enrichment analysis performed by the STRING algorithm showed that the 50 most abundant proteins in *Leishmania* exosomes of both phases, LOG and STAT, are significantly related to amino acid and protein biosynthesis processes. The main difference pointed out in this analysis was the enrichment of the energy metabolism pathways in LOG phase exosomes. One possible interpretation for this finding is that logarithmic phase parasites are in an active growth process with high energy demands, while in the stationary phase the parasites cease to duplicate and are in the process of adaptation to colonize the vertebrate host. The latter would require lower energy needs as compared to the logarithmic phase.

There are two previous studies investigating sand fly stage *Leishmania infantum* exosomes, one *in vivo* [23] and one *in vitro* [46]. The latter aligns closely with the methodology used in this present study and concerns itself with the presence of GP63 isoforms contained within these microvesicles. Additionally, and contrary to our own findings, Marshall and colleagues identified a trend of increasing GP63 from logarithmic to stationary phase exosomes. This discrepancy between this report and our own studies might be explained by a couple of methodological differences, including for example, the culture medium and parasite densities from which exosomes were derived. Their research also identified 17 GP63 isoforms across logarithmic, stationary and metacyclic populations. Our own study identified two GP63 proteins corresponding to LinJ.10.0520 (described as an isoform whose transcripts are only found in stationary phase parasites) and GP63_LEIDO and GP63_LEIAM (transcripts only found in logarithmic phase parasites). The latter is by far the most abundant GP63 we identified in both LOG and STAT exosomes. However, the two isoforms were not observed by Marshall and colleagues in logarithmic phase exosomes.

The *in vivo* study performed by Atayde and colleagues was the first verification of exosomes as a vector-transmitted virulence factor and *in vivo* exosome secretion by *Leishmania* within the sand fly midgut lumen. As expected, their analysis of the protein content of *L. infantum*

Table 3
Modulated virulence factors: Proteins modulated between exosome phases and previously associated with parasite virulence but not abundant in either exosome phase.

Modulated + Virulent				Average LFQ (Log2)		LOG/STAT
	Uniprot ID	Protein Annotation	Peptide #	LOG	STAT	Log2 LFQ Ratio
LOG	A4IAZ8	Putative casein kinase	12	27.3	26.5	0.8
	A4HUK3	Putative small GTP-binding protein Rab11	5	26.6	25.7	0.9
	A4I048	GDP-mannose pyrophosphorylase	12	27.0	25.6	1.4
	A4HW82	Putative inositol-3-phosphate synthase	11	27.1	25.4	1.7
	A4HTZ8	Oligopeptidase b	10	26.4	24.1	2.4
	A4I7B1	Iron/zinc transporter protein-like protein	2	26.6	23.4	3.2
	A4I7B5	Phosphoglycan beta 1,3 galactosyltransferase 5	9	25.3	22.7	2.6
STAT	–	–	–	–	–	–

Table 4
Abundant, Modulated virulence factors: Proteins that were abundant in at least one exosome phase, modulated between phases and previously associated with parasite virulence. EF1a, GP63 and Actin were abundant in both exosome phases.

Abdt + Mod + Vir				Average LFQ (Log2)		LOG/STAT
	Uniprot ID	Protein Annotation	Peptide #	LOG	STAT	Log2 LFQ Ratio
SHARED	A4HX73	Elongation factor 1-alpha	21	32.3	31.7	0.5
	Q6LA77	GP63	23	32.9	31.0	1.9
	A4HSC2	Actin	14	29.2	29.0	0.2
LOG	E9AHK3	S-adenosylmethionine synthase	16	29.0	26.9	2.1
	A4I993	Putative carboxypeptidase	24	28.8	26.8	2.1
	A4HYW1	Putative calpain-like cysteine peptidase	17	29.8	26.5	3.3
STAT	–	–	–	–	–	–

exosomes derived from the sand fly lumen identified a substantially lower number of proteins compared to our own *in vitro* observations. They identified three GP63 proteins, two of which were also identified in our own study. Interestingly, Atayde and colleagues identified these GP63 proteins in stationary/metacyclic stage exosomes and so, in this regard, there is concordance with the *in vitro* experiments of Marshall and colleagues. The most apparent difference between the stationary/metacyclic exosomes of Atayde and colleagues' *in vivo* study and our own *in vitro* study, is that the exosomes of the former were collected after 10–12 days of continuous sand fly infection, which would potentially mix logarithmic, stationary and metacyclic phase exosomes.

Regarding the population of Atayde and colleagues' identified proteins, 84 of the 143 proteins identified from their midgut-derived *L. infantum* exosomes were also identified in our own study. These included several cysteine peptidases, trypanothione reductase, GP63, enolase, nucleoside diphosphate kinase, peroxidoxin, HSP70 and EF1α. A total of 78 and 69 were identified in all replicates of LOG and STAT respectively, indicating there is good reason to suspect that exosomes derived from *in vivo* and *in vitro* conditions will overlap to a substantial degree.

An important aspect worth noting is the lack of research identifying the midgut-receptors that might be responsible for the uptake and dissemination of *Leishmania* exosomes within host cells. Previous research has identified trans-membrane proteins in exosomes [12] and our findings did identify some trans-membrane transport related proteins in *Leishmania* exosomes, such as ATP-binding cassette transporters [A4I4B4], cation transporters [A4I1G1, A4IBA6 and A4HSH2], and nucleoside/nucleobase transporters [A4IDG6]. If exosomes exhibit trans-membrane proteins, this may be investigated to establish the actors involved in exosome uptake.

The primary finding of this present study was the discrete grouping of LOG and STAT replicates from one another, suggesting that exosomes produced by cultured *L. infantum* are similar to that of *in vivo* parasite exosomes. Additionally, we found much overlap in the protein profiles of our culture-derived exosomes and those from previous *in vitro* and *in vivo* studies. The phase difference in protein content appears to largely consist of a drop in the number of proteins from LOG to STAT phase and a drop in the abundance of the remaining shared proteins. Due to the highly skewed nature of the protein distribution, we were unable to draw hard conclusions from the meta-analysis, and so instead, we opted to construct a system that would permit a rational identification of proteins that would be of most interest, including abundant proteins, modulated proteins and virulence factors. This has both verified previous research findings and produced new candidates for study in a context of confirmed stage-specific *Leishmania* exosome profiles. In conjunction with the sterling research conducted using vertebrate infection models, we hope the use of this proteomic data will provide new understanding and, in particular, new candidates for the targeted investigation of the growth, virulence and vulnerabilities of the etiological agent of visceral leishmaniasis in the Americas inside its' vector.

Supplementary data to this article can be found online at https://doi.org/10.1016/j.jprot.2020.103902.

Declaration of Competing Interests

After reading the BioMed Central's guidance, the authors declare no financial and non-financial competing interests.

Author contribution

Conception and design of the study: YMTC, AJT, DMF; acquisition of data: DMF; analysis and interpretation of data: DMF, MB, FKM, AJT; drafting the article or revising it critically for important intellectual content: YMTC, DMF, AJT, MB; final approval of the version to be submitted: DMF, MB, FKM, AJT, YMTC.

Acknowledgements

DMF received a doctorate fellowship from the Conselho Nacional de Desenvolvimento Científico e Tecnológico-CNPq. This work received support from the Instituto Oswaldo Cruz, Fiocruz (PAEF), and partly by the Projeto Inova, Fiocruz.

References

[1] M. Akhoundi, K. Kuhls, A. Cannet, J. Votýpka, P. Marty, P. Delaunay, et al., A historical overview of the classification, evolution, and dispersion of Leishmania parasites and Sandflies, PLoS Negl. Trop. Dis. 10 (3) (2016) 1–40.
[2] L. Gradoni, The leishmaniases: Old neglected tropical diseases, in: F. Bruschi, L. Gradoni (Eds.), The Leishmaniases: Old Neglected Tropical Diseases, 2018.
[3] J. Alvar, I.D. Vélez, C. Bern, M. Herrero, P. Desjeux, J. Cano, et al., Leishmaniasis worldwide and global estimates of its incidence, PLoS One 7 (5) (2012).
[4] P. Desjeux, Leishmaniasis: current situation and new perspectives, Comp. Immunol. Microbiol. Infect. Dis. 27 (5) (2004) 305–318 Internet. Available from http://www.sciencedirect.com/science/article/pii/S0147957104000232.
[5] J.C. Dujardin, L. Campino, C. Cañavate, J.P. Dedet, L. Gradoni, K. Soteriadou, et al., Spread of vector-borne diseases and neglect of leishmaniasis, Europe, Emerg. Infect. Dis. 14 (7) (2008) 1013–1018.
[6] PAHO, Epidemiological Report of the Americas. Rep Leishmaniases [Internet], 3 (2018), pp. 2–5. Available from http://new.paho.org/leishmaniasis.
[7] P.D. Ready, Should sand fly taxonomy predict vectorial and ecological traits? J. Vector Ecol. 36 (SUPPL.1) (2011) 17–22.
[8] D. Liu, J.E. Uzonna, The early interaction of Leishmania with macrophages and dendritic cells and its influence on the host immune response, Front. Cell Infect. Microbiol. [Internet] (2012) 2(June 2012). Available from http://journal.frontiersin.org/article/10.3389/fcimb.2012.00083/abstract.
[9] P.A. Bates, Leishmania sand fly interaction : progress and challenges, 11(4) (2008), pp. 340–344.
[10] R. Wilson, M.D. Bates, A. Dostalova, L. Jecna, R.J. Dillon, P. Volf, et al., Stage-specific adhesion of Leishmania promastigotes to sand fly midguts assessed using an improved comparative binding assay, PLoS Negl. Trop. Dis. 4 (9) (2010) 1–9.
[11] H. Mahmoodzadeh Hosseini, A. Ali Imani Fooladi, M. Reza Nourani, F. Ghanezadeh, The Role of Exosomes in Infectious Diseases, Inflamm. Allergy-Drug Targets [Internet] 12 (1) (2013) 29–37. Available from http://www.eurekaselect.com/openurl/content.php?genre=article&issn=1871-5281&volume=12&issue=1&spage=29.
[12] J.S. Schorey, Y. Cheng, P.P. Singh, V.L. Smith, Exosomes and other extracellular vesicles in host-pathogen interactions, EMBO Rep. 16 (1) (2015) 24–43 Internet. Available from http://embor.embopress.org/cgi/doi/10.15252/embr.201439363.
[13] A. Clayton, J. Court, H. Navabi, M. Adams, M.D. Mason, J.A. Hobot, et al., Analysis of antigen presenting cell derived exosomes, based on immuno-magnetic isolation

and flow cytometry, J. Immunol. Methods 247 (1) (2001) 163–174 Internet. Available from http://www.sciencedirect.com/science/article/pii/S0022175900003215.
[14] G. Raposo, H. Nijman, W. Stoorvogel, R. Liejendekker, C. Harding, C. Melief, et al., B lymphocytes secrete antigen-presentingVesicles, J. Exp. Med. 183 (March) (1996) 1161–1172.
[15] C. Théry, A. Regnault, J. Garin, J. Wolfers, L. Zitvogel, P. Ricciardi-Castagnoli, et al., Molecular characterization of dendritic cell-derived Exosomes: selective Accumunlation of the heat shock protein hsc73, J. Cell Biol. 147 (3) (1999) 599–610.
[16] J.M. Silverman, S.K. Chan, D.P. Robinson, D.M. Dwyer, D. Nandan, L.J. Foster, et al., Proteomic analysis of the secretome of Leishmania donovani, Genome Biol. 9 (2) (2008).
[17] J.M. Silverman, J. Clos, C.C. De'Oliveira, O. Shirvani, Y. Fang, C. Wang, et al., An exosome-based secretion pathway is responsible for protein export from Leishmania and communication with macrophages, J. Cell Sci. 123 (6) (2010) 842–852 Internet. Available from http://jcs.biologists.org/lookup/doi/10.1242/jcs.056465.
[18] B. Pérez-cabezas, N. Santarém, P. Cecílio, C. Silva, J.A.M. Catita, A. Cordeiro, et al., More than just exosomes : distinct Leishmania infantum extracellular products potentiate the establishment of infection potentiate the establishment of infection, J Extracell Vesicles [Internet] 8 (1) (2019), https://doi.org/10.1080/20013078.2018.1541708 Available from.
[19] J.M. Silverman, N.E. Reiner, Leishmania Exosomes deliver Preemptive strikes to create an environment permissive for early infection, Front. Cell Infect. Microbiol. [Internet]. 1 (January) (2012) 1–8. Available from: http://journal.frontiersin.org/article/10.3389/fcimb.2011.00026/abstract.
[20] J.M. Silverman, J. Clos, E. Horakova, A.Y. Wang, M. Wiesgigl, I. Kelly, et al., , Leishmania Exosomes modulate innate and adaptive immune responses through effects on monocytes and dendritic cells, J. Immunol. 185 (9) (2010) 5011–5022 Internet. Available from http://www.jimmunol.org/cgi/doi/10.4049/jimmunol.1000541.
[21] M.T. Shio, J.G. Christian, J.Y. Jung, K.P. Chang, M. Olivier, PKC/ROS-mediated NLRP3 inflammasome activation is attenuated by leishmania zinc- metalloprotease during infection, PLoS Negl. Trop. Dis. 9 (6) (2015) 1–21.
[22] R. Belo, N. Santarém, C. Pereira, B. Pérez-Cabezas, F. Macedo, M. Leite-de-Moraes, et al., Leishmania infantum exoproducts inhibit human invariant NKT cell expansion and activation, Front. Immunol. 8 (JUN) (2017).
[23] V.D. Atayde, H. Aslan, S. Townsend, K. Hassani, S. Kamhawi, M. Olivier, Exosome Secretion by the Parasitic Protozoan Leishmania within the Sand Fly Midgut, Cell Rep [Internet] 13 (5) (2015) 957–967. Available from https://doi.org/10.1016/j.celrep.2015.09.058.
[24] G. Dong, A. Lira Filho, M. Olivier, Modulation of host-pathogen communication by extracellular vesicles (EVs) of the protozoan parasite ***Leishmania***, Front. Cell. Infect. Microbiol. 9 (2019) 100.
[25] E.L. Telleria, M.R. Sant'Anna, J.R. Ortigão-Farias, A.N. Pitaluga, V.M. Dillon, P.A. Bates, Y.M. Traub-Csekö, R.J. Dillon, Caspar-like gene depletion reduces Leishmania infection in sand fly host Lutzomyia longipalpis, J. Biol. Chem. 287 (16) (2012 Apr 13) 12985–12993.
[26] E.L. Telleria, M.R. Sant'Anna, M.O. Alkurbi, A.N. Pitaluga, R.J. Dillon, Y.M. Traub-Csekö, Bacterial feeding, *Leishmania* infection and distinct infection routes induce differential defensin expression in *Lutzomyia longipalpis*, Parasit. Vectors (2013 Jan 11)https://doi.org/10.1186/1756-3305-6-12 6:12.
[27] B. Tinoco-Nunes, E.L. Telleria, M. da Silva-Neves, C. Marques, D.A. Azevedo-Brito, A.N. Pitaluga, Y.M. Traub-Csekö, The sandfly Lutzomyia longipalpis LL5 embryonic cell line has active toll and Imd pathways and shows immune responses to bacteria, yeast and *Leishmania*, Parasit. Vectors 9 (2016 Apr 20) 222.
[28] A. Martins-da-Silva, E.L. Telleria, M. Batista, F.K. Marchini, Y.M. Traub-Csekö, A.J. Tempone, Identification of secreted proteins involved in nonspecific dsRNA-mediated Lutzomyia longipalpis LL5 cell antiviral response, Viruses 10 (1) (2018) 1–17.
[29] C. Bordier, R.J. Etges, J. Ward, M.J. Turner, M.L. Cardoso de Almeida, Leishmania and Trypanosoma surface glycoproteins have a common glycophospholipid membrane anchor, Proc. Natl. Acad. Sci. U. S. A. 83 (16) (1986) 5988–5991.
[30] C. Yao, J.E. Donelson, M.E. Wilson, The major surface protease (MSP or GP63) of Leishmania sp. biosynthesis, regulation of expression, and function, Mol. Biochem. Parasitol. 132 (1) (2003) 1–16.
[31] B.S. McGwire, K.P. Chang, D.M. Engman, Migration through the extracellular matrix by the parasitic protozoan Leishmania is enhanced by surface metalloprotease gp63, Infect. Immun. 71 (2) (2003) 1008–1010.
[32] G. Chaudhuri, M. Chaudhuri, A. Pan, K.P. Chang, Surface acid proteinase (gp63) of Leishmania mexicana. A metalloenzyme capable of protecting liposome-encapsulated proteins from phagolysosomal degradation by macrophages, J. Biol. Chem. 264 (13) (1989) 7483–7489.
[33] A. Sorensen, A.S. Hey, K. Arsalan, Leishmania major surface protease Gp63 interferes with the function of human monocytes and neutrophils in vitro, APMIS [Internet] 102 (1–6) (1994 May 30) 265–271. Available from https://doi.org/10.1111/j.1699-0463.1994.tb04874.x.
[34] T. Lieke, S. Nylén, L. Eidsmo, W.R. McMaster, A.M. Mohammadi, A. Khamesipour, et al., Leishmania surface protein gp63 binds directly to human natural killer cells and inhibits proliferation, Clin. Exp. Immunol. 153 (2) (2008) 221–230.
[35] Olivier M, Atayde VD, Isnard A, Hassani K, Shio MT. Leishmania virulence factors: Focus on the metalloprotease GP63. Microbes Infect [Internet]. 2012;14(15):1377–89. Available from: doi:https://doi.org/10.1016/j.micinf.2012.05.014.
[36] M. Olivier, D.J. Gregory, G. Forget, Subversion mechanisms by which Leishmania parasites can escape the host immune response : a Signaling point of view subversion mechanisms by which leishmania parasites can escape the host immune response : a signaling point of view, Clin. Microbiol. Rev. 18 (2) (2005) 293–305.
[37] M.T. Shio, K. Hassani, A. Isnard, B. Ralph, I. Contreras, M.A. Gomez, et al., Host cell signalling and leishmania mechanisms of evasion, J. Trop. Med. 2012 (2012).
[38] M.M. Kulkarni, W.R. McMaster, E. Kamysz, W. Kamysz, D.M. Engman, B.S. McGwire, The major surface-metalloprotease of the parasitic protozoan, Leishmania, protects against antimicrobial peptide-induced apoptotic killing, Mol. Microbiol. 62 (5) (2006) 1484–1497.
[39] R.P. Soares, E.C.F. Altoé, V. Ennes-Vidal, S.M. da Costa, E.F. Rangel, N.A. de Souza, et al., In Vitro Inhibition of Leishmania Attachment to Sandfly Midguts and LL-5 Cells by Divalent Metal Chelators, Anti-gp63 and Phosphoglycans, Protist [Internet] 168 (3) (2017) 326–334. Available from https://doi.org/10.1016/j.protis.2017.03.004.
[40] E.L. Telleria, A. Martins-da-Silva, A.J. Tempone, Y.M. Traub-Csekö, *Leishmania*, microbiota and sand fly immunity, Parasitology 145 (10) (2018 Sep) 1336–1353.
[41] D. Nandan, T. Yi, M. Lopez, C. Lai, N.E. Reiner, Leishmania EF-1α activates the Src homology 2 domain containing tyrosine phosphatase SHP-1 leading to macrophage deactivation, J. Biol. Chem. 277 (51) (2002) 50190–50197.
[42] W. Robert McMaster, C.J. Morrison, M.S. Kobor, Epigenetics: A New Model for Intracellular Parasite-Host Cell Regulation, Trends Parasitol. [Internet] 32 (7) (2016) 515–521. Available from https://doi.org/10.1016/j.pt.2016.04.002.
[43] Braga Micheline, Leandro Xavier Nevesa, Jonatan Marques Camposa, Bruno Mendes Roatt, Rodrigo Dian de Oliveira Aguiar Soares, Samuel Leôncio Braga, Daniela de Melo Resende, Alexandre Barbosa Reis, William Castro-Borges, Shotgun proteomics to unravel the complexity of the Leishmania infantum exoproteome and the relative abundance of its constituents, Molecular and biochemical Parasitology 195 (2014) 43–53, https://doi.org/10.1016/j.molbiopara.2014.07.001 In press.
[44] M.C. Duarte, D.C. Pimenta, D. Menezes-Souza, R.D.M. Magalhães, J.L.C.P. Diniz, L.E. Costa, et al., Proteins selected in Leishmania (Viannia) braziliensis by an immunoproteomic approach with potential serodiagnosis applications for tegumentary leishmaniasis, Clin. Vaccine Immunol. 22 (11) (2015) 1187–1196.
[45] I. Abu-Dayyeh, K. Hassani, E.R. Westra, J.C. Mottram, M. Olivier, Comparative study of the ability of Leishmania mexicana promastigotes and amastigotes to alter macrophage signaling and functions, Infect. Immun. 78 (6) (2010) 2438–2445.
[46] S. Marshall, P.H. Kelly, B.K. Singh, R.M. Pope, P. Kim, B. Zhanbolat, et al., Extracellular release of virulence factor major surface protease via exosomes in Leishmania infantum promastigotes, Parasit. Vectors 11 (1) (2018) 1–10.